https://doi.org/10.5194/bg-2021-296
Preprint. Discussion started: 11 November 2021

Biogeosciences Discussions Open Access EGU

Variations in and environmental controls of primary productivity in the Amundsen Sea

Jianlong Feng [1], Delei Li [2,3], Jing Zhang[1], Liang Zhao [1]*

[1] Key Laboratory of Marine Resource Chemistry and Food Technology (TUST), Ministry of Education, Tianjin University of Science and Technology, Tianjin 300457, China

[2] CAS Key Laboratory of Ocean Circulation and Waves, Institute of Oceanology, Chinese Academy of Sciences, Qingdao, China

[3] Center for Ocean Mega-Science, Chinese Academy of Sciences, Qingdao, China

*Corresponding author, Key Laboratory of Marine Resource Chemistry and Food Technology (TUST), Ministry of Education, Tianjin University of Science and Technology, Tianjin 300457, PR China. Telephone number: 86-18698004519, Email address: zhaoliang@tust.edu.cn

Abstract: The Amundsen Sea is one of the regions with the highest primary productivity in the Antarctic. To better understand the role of the Southern Ocean in the global carbon cycle and in climate regulation, a better understanding of the variations in and environmental controls of primary productivity is needed. Using cluster analysis, the Amundsen Sea was divided into nine bioregions. The biophysical differences among bioregions enhanced confidence to identify priorities and regions to study the temporal and spatial variations in primary productivity. Four nearshore bioregions with high net primary productivity or rapidly increasing rates were selected to analyze

https://doi.org/10.5194/bg-2021-296
Preprint. Discussion started: 11 November 2021

temporal and spatial variations in primary productivity in the Amundsen Sea. Due to changes in net solar radiation and sea ice, primary production had significant seasonal variation in these four bioregions. The phenology had changed at two bioregions (3 and 5), which has the third and fourth highest primary production, due to changes in the dissolved iron, nitrate, phosphate, and silicate concentrations. Annual primary production showed increasing trends in these four bioregions. The variation in primary production in the bioregion (9), which has the highest primary production, was mainly affected by variations in sea surface temperatures. In the bioregion, which has the second-highest primary production (8), the primary production was significantly positively correlated with sea surface temperature and significantly negatively correlated with sea ice thickness. The long-term changes of primary productivity in bioregions 3 and 5 were thought to be related to changes in the dissolved iron, nitrate, phosphate, and silicate concentrations, and dissolved iron was the limiting factor in these two bioregions. Bioregionalization not only disentangle multiple factors that control the spatial differences, but also disentangle limiting factors that affect the phenology, decadal and long-term changes in primary productivity.

Keywords: Amundsen Sea; primary productivity; bioregions; dissolved iron

Plain Language Summary

Although some studies have been conducted on primary productivity in the Amundsen Sea, it is still one of the least studied regions in the Southern Ocean. The spatial differences and mechanisms that drive differences in phenology, decadal and long-term changes in primary productivity are still not clear. In this work, we used

https://doi.org/10.5194/bg-2021-296
Preprint. Discussion started: 11 November 2021

bioregionalization to provide a basis for understanding variations in primary productivity in the Amundsen Sea. Due to changes in the dissolved iron, nitrate, phosphate, and silicate concentrations, the phenology of primary production had changed at two bioregions, which has third and fourth highest primary production (3 and 5). Annual primary production showed increasing trends from 1993 to 2015 in 4 near shore bioregions due to changes in SST, sea ice, and dissolved iron. The dissolved iron was thought to be the limiting factor of long-term change in two bioregions 3 and 5. Bioregionalization was proven to be an effective method to disentangle multiple limiting factors that affect spatial differences, the phenology, decadal and long-term changes in primary productivity.

Introduction

The Southern Ocean, also known as the Antarctic Ocean, encompasses 10% of the global ocean and contains parts of the South Pacific Ocean, the South Atlantic Ocean, the South Indian Ocean, and the marginal seas around Antarctica, such as the Ross Sea, Weddell Sea, and the Amundsen Sea. The Southern Ocean contains 40% of the total oceanic inventory of anthropogenic carbon dioxide (Khatiwala et al., 2009), and plays an important role in Earth's climate regulation, especially by neutralizing the effects of rising carbon dioxide concentrations and rising global temperatures (Reid et al., 2009; Ma et al., 2012; Bijma et al., 2013; Petrou et al., 2016). The Amundsen Sea lies between the Cape Flying Fish and Cape Dart on Slip Island, and is one of the most rapidly

https://doi.org/10.5194/bg-2021-296
Preprint. Discussion started: 11 November 2021

warming regions on Earth (Figure 1) (Bromwich et al., 2013), and it is one of the least studied Antarctic continental shelf regions (Griffiths 2010; Pabis et al., 2014).

Primary productivity plays an important role in the transformation of dissolved elements in the ocean and in ocean-atmosphere carbon exchange (Amthor and Baldocchi, 2001). Previous studies have indicated that the phenology, decadal and long-term changes in primary productivity in the Southern Ocean have been and will continue to be affected by the current and predicted changes in ocean circulation and hydrology associated with climate variability (Lannuzel et al., 2007; Herraiz-Borreguero et al., 2016; Kim and Kim, 2021). Significant spatial differences exist in the changes in primary productivity in the Southern Ocean, both over large latitudinal scales and at regional scales (Arrigo et al., 2008; Ardyna et al., 2017). These spatial differences are related to nutrient availability (mainly iron and possibly nitrate and silicic acid), temperature, light availability, and mortality factors (Boyd, 2002; Behernfeld and Boss, 2014; Arrigo et al., 2015). These factors are controlled by vertical mixing, advection, sea ice cover, and seasonal variations in solar irradiance (Ardyna et al., 2017). However, studies of the primary productivity of the Southern Ocean have been limited in their ability to assess spatial variabilities over both short and long timescales for a variety of different reasons (Arrigo et al., 2008). Primary productivity also shows significant spatial differences in the Amundsen Sea, the Amundsen Sea Polynya is the region of particularly high productivity in the Southern Ocean (Arrigo and van Dijken, 2003; Lee et al., 2012). Although some studies have been conducted on primary productivity in the Amundsen Sea (Arrigo and van Dijken, 2003; Arrigo et

https://doi.org/10.5194/bg-2021-296
Preprint. Discussion started: 11 November 2021

al., 2012; Lee et al., 2012; Park et al., 2017; Lim et al., 2019; Kwon et al., 2021), the spatial differences and mechanisms that drive differences in phenology, decadal and long-term changes in primary productivity are still not clear.

Bioregionalization is one method used to define ecosystems. Under this approach, regions are defined based on physical and biological properties, the method can be defined as the process of delineating the continuous spatial coverage of contiguous spatial units that support distinct biological assemblages (Costello, 2009; Koubbi et al., 2011; Roberson et al., 2017). Usually, the spatial units are delineated using geophysical and biological observation data, modeled data, or a combination of both (Grantham et al., 2010). The obtained bioregions can be used for monitoring and reporting the state of the environment, modeling and predicting the effects of climate changes and identifying priority areas for protection (Gregr and Bodtker, 2007; Spalding et al., 2007; Rice et al.., 2011). In recent years, the delimitation of marine bioregions has also been used to disentangle multiple limiting factors that affect the efficiency of biological pumps mediated by phytoplankton (Longhurst, 2007; Ardyna et al., 2017), the spatial and temporal changes of key ecological parameters (Bowman et al., 2018). In the Southern Ocean, bioregionalization has been widely used to identify representative areas for protection at broad and regional scales, such as in Southern Ocean (Grant et al., 2006), Ross Sea region (Sharp et al., 2010), and Weddell Sea (Teschke et al., 2016). Delineating the effects of environmental forcing on temporal and spatial variations in primary productivity remains challenging and requires novel approaches. We used bioregionalization to provide a basis for understanding variations in primary

https://doi.org/10.5194/bg-2021-296
Preprint. Discussion started: 11 November 2021

productivity in the Amundsen Sea.

In this paper, we conducted a cluster analysis using variables from the Global Ocean Reanalysis and Simulations (GLORYS) dataset to obtain a bioregional map of the Amundsen Sea. Using the bioregionalization outputs, we analyzed the limiting factors that affect spatial differences, the phenology, decadal and long-term changes in primary productivity in the Amundsen Sea.

2. Data and Methodology

2.1 Data

The physical and ecological variables used in the bioregionalization were derived from the Global Ocean Reanalysis and Simulation Version 4 (GLORYS2v4) dataset (https://resources.marine.copernicus.eu/?option=com_csw&task=results&pk_vid=f205f72451b76b161622075614d28a7a). GLORYS2v4 is an ocean reanalysis, which is a scientific method that produces a comprehensive records of how ocean properities are changing over time. This reanalysis is performed with NEMOv3.1 ocean model in configuration ORCA025_LIM. The vertical grid has 75 levels with partial steps at the bottom. GLORYS2v4 has assimilated observations, containing delayed time along-track satellite Sea Level Anomaly, Sea Ice Concentration, Sea Surface Temperature, and in situ profiles of temperature and salinity from CORA4 database. The monthly mean values from 1993 to 2015 with a resolution of 1/4 °×1/4 °were used in this work. *In situ* observed temperature and salinity data were acquired during the *ANTXXVI/3* from the research ice breaker Polarstern (Gohl, 2010). The Climate Data Record (CDR)

https://doi.org/10.5194/bg-2021-296
Preprint. Discussion started: 11 November 2021

of sea ice concentration from obtained from NSIDC (Meier et al., 2017). Chlorophyll-a data were obtained from the Ocean Colour Climate Change Initiative (OC-CCI, http://www.esa-oceancolour-cci.org) project.

Previous studies have shown that variables obtained from GLORY2v4 perform well against observations in the Amundsen Sea (Uotlia et al., 2019; Huang et al., 2020). In this work, we also compare the temperature, salinity, sea ice concentration, and chlorophyll against observations in the Amundsen Sea (shown in Supplementary Figure S1-S3). Results showed that comparisons between the GLORYS2v4 and in situ / satellite measurements of the temperature, salinity, sea ice concentration, and chlorophyll show a good agreement. Also, the mixed layer depths were calculated according to Patel (2021) at the S01 section (Figure S1). The mixed layer depths obtained from the observations ranged from 4 to 24 m with a mean of 15 m. At the same time, the mixed layer depths obtained from GLORYS2v4 ranged from 5 to 27 m with a mean of 17m. The above results enhanced the confidence in the quality of the GLORYS2v4 to get the bioregions in the Amundsen Sea.

As variables measured at the ocean surface are strongly correlated with processes at depth, the surface variables can reflect the properties of the water column (Longhurst, 2007; Oliver and Irwin, 2008). Therefore, the variables of the first layer were used in this work. The extents of all variables were clipped to match the study area, ranging from 80 °to 150 °W and 55 °to 80 °S. In addition to total primary production of phytoplankton (nppv in table 1), other physical and biological variables were also selected. These variables were selected according to two principles: first, variables

https://doi.org/10.5194/bg-2021-296
Preprint. Discussion started: 11 November 2021

153 selected by other studies conducted in the Southern Ocean were also selected in this
154 work, including the sea surface temperature (SST), sea surface height (SSH), salinity,
155 water depth, sea ice persistence index, sea bottom temperature, and chlorophyll (Table
156 1); second, variables that could affect primary productivity were also selected,
157 including the mixed layer depth, and dissolved iron (Table 1). The parameters used in
158 the clustering analysis contained the average states of the variables (mean value across
159 the time series), their variability (annual maximum mean, annual minimum mean, long-
160 term change rate), and topographic gradient. The sea ice persistence index was
161 calculated from the proportion of the overall time during which the grid was covered
162 by sea ice. All variables were standardized to zero means and unit standard deviations
163 to eliminate issues associated with units of measurement.

164 **2.2 Methodology**

165 Bioregions were obtained in this work using cluster methods. Cluster analysis is a class
166 of techniques in which a set of objects or cases classified in the same group (called a
167 cluster) are more similar to each other than to those in other groups. One advantage of
168 cluster techniques is that they allow for areas with similar characteristics to be defined
169 regardless of their location, thereby producing results representative of intrinsic spatial
170 patterns and environmental variables (Leathwick et al., 2003; Snelder et al., 2007).
171 Cluster analysis has been commonly used to identify bioregions and is still widely used
172 today (Milligan and Cooper, 1987; Ebach et al., 2015; Roberson et al., 2017;
173 Bloomfield et al., 2018). For the Southern Ocean, physical and biological variables,

https://doi.org/10.5194/bg-2021-296
Preprint. Discussion started: 11 November 2021

including the water temperature, salinity, depth, chlorophyll, and sea-ice information, were used to obtain the bioregions to facilitate systematic planning for the protection of marine habitat diversity (Grant et al., 2006; Sharp et al., 2010; Teschke et al., 2016; Godet et al., 2020).. In this work, hierarchical clustering and the *K*-means clustering method were selected to obtain bioregions in the Amundsen Sea. *K*-means clustering is a data-mining method that classifies objects into *K* clusters, objects within a given cluster are more similar to each other (in the multivariate space) than to those in other clusters. This approach has been successfully applied in the North Atlantic (Lacour et al., 2015), the Southern Ocean (Ardyna et al., 2017), and the Mediterranean Sea (Mayot et al., 2016; Palmi éri et al., 2018) as well as at the global scale (D'Ortenzio et al., 2012). The number of *K* categories used for the *K*-means clustering was determined using the hierarchical clustering method, which depends on the pairwise distances between data points to merge or divide data into a series of clusters (Fraley and Raftery, 1998).

3. Results and Discussion

3.1 Primary productivity in the Amundsen Sea

The mean value (Figure 2A) and seasonality amplitude (Figure 2B) of primary production in the Amundsen Sea were calculated using the data obtained from GLORYS2V4. The spatial differences were quite significant in the Amundsen Sea, and the mean primary production values of the Amundsen Sea ranged from 1.5 to 14 mgC m^{-3} day^{-1}. In most areas, the mean value was less than 3 mgC m^{-3} day^{-1}. The primary

https://doi.org/10.5194/bg-2021-296
Preprint. Discussion started: 11 November 2021

195 production was largest in Pine Island Bay, and minimum values occurred on the two
196 areas adjacent to of Pine Island Bay, with a mean value of less than 2 mgC m^{-3} day^{-1}.
197 This distribution was consistent with other studies about primary production in the
198 Amundsen Sea (Park et al., 2019). The seasonality amplitude of primary production
199 (Figure 2B) ranged from 10 to 100 mgC m^{-3} day^{-1} and showed some similar spatial
200 characteristics with the mean values, the amplitude was also largest in Pine Island Bay.
201 However, the spatial variations in the seasonality amplitude were more complicated
202 than those of the mean value. The seasonality amplitude was not the smallest in the two
203 areas adjacent to Pine Island Bay, featuring a mean value less than 2 mgC m^{-3} day^{-1}.
204 The annual primary production showed an increasing trend from 1993 to 2015 (Figure
205 2C). The primary production was relatively large from 2000 to 2006; reached a
206 maximum in 2004, and displayed low values from 1993 to 1996; a minimum occurred
207 in 1994. Furthermore, the progressive *UF(t)* and the retrograde *UB(t)* series of the
208 sequential Mann-Kendall test (Mann, 1945; Kulkarni and von Storch, 1999) were
209 calculated against time for the annual mean primary production (Figure 2D). The results
210 showed that primary production featured an increasing trend in general. The positive
211 trend was significant after 1999, and no mutation existed in the annual primary
212 production. Primary production exhibited clear seasonal variability (Figure 2E), it
213 began to increase in August, reached a maximum in December, and began to decrease
214 after December. From April to September, the primary production was less than 2 mgC
215 m^{-3} day^{-1}. The monthly primary production varied greatly in the summer months, and
216 the amplitude was largest in December (ranging from 4.5 to 14.5 mgC m^{-3} day^{-1}). Above

https://doi.org/10.5194/bg-2021-296
Preprint. Discussion started: 11 November 2021

results were in consistent with previous studies using observations (Arrigo and van Dijken, 2003; Park et al., 2017; Lim et al., 2019; Kwon et al., 2021),and enhanced the confidence in the data quality and in the analysis.

3.2 Bioregion classification and characterization

To obtain the number of clusters (*K*), hierarchical clustering was carried out in the Amundsen Sea. The dendrogram obtained from the hierarchical clustering algorithm was used to guide the clustering process (Figure 3). Norse (2010) indicated that if *K* is too large, important details are overlooked; if K is too small, the result is an unmanageable number of decision-making groups. To obtain a more reasonable result, *K*-means cluster analyses were carried out twice (*K*=6 and *K*=9) (Figure 4). The results (Figure 4) show that spatial distribution had similar characteristics between the *K*=6 and *K*=9 results. But differences also existed, when *K*=9 was selected, the coastal area was divided into 2 bioregions (9-8 and 9-9). When *K*=6 was selected, the coastal area was divided into 1 bioregion (6-6). The northern boundary area was divided into two bioregions (6-2 and 6-3) when *K*=6, while it was divided into three bioregions (9-4, 9-6, and 9-7) when *K*=9. When *K*=6, the central region was divided into two bioregions (6-1 and 6-2), and when *K*=9, the central region was divided into three bioregions (9-1, 9-2, and 9-3). For comparison, the mean values of the variables in different bioregions were calculated (6-6, 9-8 and 9-9; 6-3, 9-4, and 9-7) (Table 2). The results showed that the differences in the physical variables were small among bioregions 6-6, 9-8, and 9-

https://doi.org/10.5194/bg-2021-296
Preprint. Discussion started: 11 November 2021

9, while the differences in the biological variables were quite pronounced. The mean values of *chl* and *nppv* were significantly smaller in the 9-8 bioregion than those in the 6-6 and 9-9 bioregions. The differences in biological variables among bioregions 6-3, 9-4, and 9-7 were small, while the differences in physical variables were quite clear, especially the *mlp*, *ssh*, and *fice* variables. The above results indicated that the bioregions obtained from K=9 can describe the detailed differences in *fice*, *mlp*, *chl* and *nppv* more clearly than the bioregions obtained from K=6. All these variables are important in a spatial analysis of primary production in the Amundsen Sea; therefore, we ultimately selected the resulting bioregions when K=9.

The parameters that characterize the key properties of each bioregion differed among the bioregions (Figure 5). Here, we listed four levels of each parameter to help characterize each bioregion relative to the study area: the maximum value, the second-highest value, the minimum value, and the second-lowest value. Bioregions 8 and 9 are associated with the continental shelf and slope edge down to approximately 300 m. The Amundsen Sea Polynya is located in this region (Swalethorp et al., 2019), and these two bioregions are the areas through which the coastal current flows in the Amundsen Sea (Kim et al., 2016). Bioregions 8 and 9 showed some similar features; they were both distinguished by low *tem*, low *mlp*, low *sal*, high *chl*, high *nppv*, high *fe*, and low *dep* values. There were also some differences between bioregions 8 and 9; bioregion 9 had the lowest *bot* value, while bioregion 8 had the second-highest *bot* value. The *fice* values of bioregion 8 were higher than those of bioregion 9, the *tem* values of bioregion 8 were lower than those of bioregion 9, bioregion 9 had the second-highest longitudinal

https://doi.org/10.5194/bg-2021-296
Preprint. Discussion started: 11 November 2021

gradient, and bioregion 8 had the second-lowest latitudinal gradient. Although bioregion 8 had the second-highest *nppv* value, the *nppv* value of bioregion 9 (8.51 mgC m^{-3} day^{-1}) was much higher than that of bioregion 8 (5.86 mgC m^{-3} day^{-1}). Bioregion 5 was located within the continental slope, and its boundary was mostly consistent with the Antarctic Slope Front (Martinson, 2012). Bioregion 5 was distinguished by the lowest *tem*, lowest *mlp*, second-lowest *ssh*, highest *bot*, highest *fice*, lowest *chl*, and lowest *nppv*, vaules and the lowest latitudinal gradient and highest longitudinal gradient. In this bioregion, Circumpolar Deep Water (CDW) intrudes onto the shelf, after which it mixes with surrounding water and masses to become Modified Circumpolar Deep Water (MCDW) (Arneborg et al., 2012; Stalaurent et al., 2017). MCDW is a potential source of dissolved iron fueling primary productivity in bioregions 8 and 9 (St-Laurent et al., 2017; Dinniman et al., 2020).

Bioregions 1, 2, 3, 4, 6, and 7 were located in the abyssal plain. Bioregion 3 was distinguished by the second-lowest *mlp*, the lowest *ssh* and the second-lowest *chl* and *nppv* values. Bioregion 3 was therefore assumed to be closely associated with the Ross Gyre (Dotto et al., 2018). The Ross Gyre is formed by the interaction between the Antarctic Circumpolar Current and the Antarctic Continental Shelf and rotates clockwise. The northern boundary of bioregion 1 mostly consisted of winter sea ice (Comiso et al., 2003). Bioregion 2 was distinguished by the second-lowest *bot*, the second-lowest *fe*, and the second-lowest annual maximum *chl* values. The sea ice of bioregion 2 decreased from 1993 to 2015, and the rate of sea ice decrease was the largest in bioregion 2 among all bioregions. Bioregions 4, 6, and 7 were located at the northern

https://doi.org/10.5194/bg-2021-296
Preprint. Discussion started: 11 November 2021

boundary of the study region, and these bioregions are the areas through which Antarctic Circumpolar Current flows. Bioregion 6 was distinguished by the highest *tem*, the highest *mlp*, the highest *ssh*, the lowest *fice*, the highest *sal* and the lowest *dep* values. Bioregion 4 was distinguished by the second-highest *tem*, the second-highest *mlp*, the second-highest *ssh*, the second-lowest *fice*, the second-highest *sal*, and the second-lowest *dep* values. Bioregion 7 was distinguished by the lowest *fe* value the lowest longitudinal gradient, and the lowest long-term change rate of *tem.*

The above results indicated that the bioregions differed in their physical and biological characteristics (including primary productivity). These bioregions can be used to study the temporal and spatial variations in primary productivity in the Amundsen Sea. Furthermore, the 9 bioregions had biophysical significance; therefore, they are also useful for systematic conservation planning of marine protected areas (MPAs) in the Amundsen Sea (Fraschetti et al., 2008; Treml and Halpin, 2012).

3.3 Variations in primary productivity

In the Amundsen Sea, intense phytoplankton blooms occasionally develop, making primary productivity highly variable both temporally and spatially (Moore and Abbott, 2000; Arrigo et al., 2008) (Figure 2B). Our results outlined in section 3.2 indicated that the 9 obtained bioregions can be used to reflect the temporal differences in primary productivity in the Amundsen Sea. The mean value, annual maximum mean, and long-term change rate of primary production were calculated in the 9 bioregions and are

https://doi.org/10.5194/bg-2021-296
Preprint. Discussion started: 11 November 2021

303 shown in Figure 6. The results showed that the mean and annual maximum mean values
304 of primary production in bioregions 8 and 9 were significantly larger than those in other
305 bioregions. This is because the polynyas in the Amundsen Sea are located in bioregion
306 8 and 9. The long-term change rate of bioregion 9 was the largest, followed by those of
307 bioregions 3 and 5. Therefore, bioregions 3, 5, 8, and 9 were selected as typical
308 bioregions with which to analyze variations in primary productivity in the Amundsen
309 Sea.
310 Primary productivity exhibited clear seasonal variability in these four bioregions
311 (Figure 7). The primary production was large from November to March, and the
312 monthly variations were more significant in bioregions 8 and 9 than in the other
313 bioregions. From April to October, the differences among these 4 bioregions became
314 small, and primary production in these 4 bioregions was less than 1 mgC m^{-3} day^{-1}.
315 Seasonal variations in primary productivity in the Amundsen Sea were mainly caused
316 by changes in net solar radiation, sea ice, and iron (Moore and Abbott, 2000;
317 Stammerjohn et al., 2015; Wu and Hou, 2017; St-Laurent et al., 2019). In the Amundsen
318 Sea, the sea ice coverage increased after March and reached a maximum value in austral
319 winter (Figure 8). After September, the sea ice coverage decreased and reached a
320 minimum value in austral summer. The production of meltwater, the generation of a
321 stratified surface layer, and the release of biogenic elements (such as iron) increased
322 phytoplankton growth and accumulation within the marginal ice zone (Ritterhoff and
323 Zauke, 1997; Smith Jr and Comiso, 2008; St-Laurent et al., 2019). The net solar
324 radiation of the Southern Ocean has significant seasonal variations and is higher in

https://doi.org/10.5194/bg-2021-296
Preprint. Discussion started: 11 November 2021

325 spring (September to November) and summer (December to February) and lower in
326 autumn (March to May) and winter (June to August). At the same time, sea ice coverage
327 can regulate the availability of irradiance to phytoplankton in the Amundsen Sea. Under
328 the effects of polar night and large sea ice coverage, the primary production was close
329 to 0 from May to September in these four bioregions. Results also showed that the
330 dissolved iron also exhibited clear seasonal variability. The iron reached a maximum in
331 November, and then decreased, it reached its minimum in February (Figure 8). Previous
332 studies of the coastal polynya also found that the phytoplankton bloom is primarily
333 light-limited in its early stages, but as the pool of dissolved iron is depleted by
334 phytoplankton uptake, there is a transition towards iron limitation (St-Laurent et al.,
335 2019; Twelves et al., 2020).
336 The results also showed that the phenology changed over the study period in bioregions
337 3 and 5 (Figure 9). In bioregion 3, primary production reached a maximum in January
338 before 1998, while after 1998, maximum primary production occurred in December. In
339 bioregion 3, the primary production rates in November and December increased
340 significantly after 1998. In bioregion 5, primary production reached its maximum in
341 January before 2001; after 2001, the maximum primary production occurred in
342 December. In bioregion 5, primary production increased significantly in November and
343 December after 2001. These variations in primary production in bioregions 3 and 5
344 were thought to be related to the changes in iron, nitrate, phosphate, and silicate (Figure
345 10). The melting of the ice shelf increases iron availability due to the meltwater pump
346 effect and due to the release of iron entrained at the glacier bed (Twelves et al., 2021).

https://doi.org/10.5194/bg-2021-296
Preprint. Discussion started: 11 November 2021

In bioregion 3, the dissolved iron concentrations increased significantly in November and December after 1998; these increased values were more than 2 times higher than those recorded before 1998. Alderkamp et al. (2015) indicated that primary productivity would be stressed by low iron concentrations during December and January in the Amundsen Sea. Increased dissolved iron concentrations resulted in increased primary production in November and December after 1998. In bioregion 5, the dissolved iron concentrations also increased in November and December after 1998, and the nitrate, phosphate, and silicate concentrations increased significantly in November and December after 2000. The changes in dissolved iron, nitrate, phosphate, and silicate resulted in increased primary production in November and December after 2000. Kwon et al. (2021) also found that the increase in iron can lead to a shift in the bloom peak timing to earlier than January in the Amundsen Sea continental shelf water (mostly in bioregion 5) using a 1-D pelagic ecosystem model.

The changes in primary production from 1993 to 2015 in bioregions 3, 5, 8, and 9 were also analyzed (Figure 11). The results showed that primary production showed positive linear trends in these four bioregions, and these trends were significant at the 95% confidence level in bioregions 3, 5, and 9. Bioregion 9 had the fastest growth rate, and the decadal variations in bioregion 9 were also larger than those in the other 3 bioregions. Primary production reached highest in 2006 and was relatively low in 1994, 1999, 2000, and 2015. The increasing trend observed in bioregion 8 was not significant, but the interannual variations were more significant in bioregion 8 than those in bioregions 3 or 5. The interannual and decadal variations between bioregion 8 and

https://doi.org/10.5194/bg-2021-296
Preprint. Discussion started: 11 November 2021

bioregion 9 were quite similar, with a correlation coefficient of approximately 0.75 (calculated using the time series after long-term trend removal). In bioregion 9, a significant positive correlation existed between primary production and sea surface temperatures in summer (from November to March), and the correlation coefficient was 0.46. In bioregion 8, the interannual and decadal variations in primary production were positively correlated with the sea surface temperature in summer, and the correlation coefficient was 0.45. These variations in primary production were also significantly negatively correlated with sea ice thickness, and the correlation coefficient was -0.54. Therefore, the changes in primary production recorded in bioregions 8 and 9 may have been caused by changes in the sea surface temperatures in summer in these areas. Previous studies have shown that SSTs can impact rates of products directly through the relationship between temperature and phytoplankton metabolic rate; SSTs can also affect surface ocean stratification and sea ice distributions (Arrigo et al., 2008). The decline in sea ice thickness can increase the light availability, which has significant effects on the blooms in the nearshore and coastal polynyas in the Amundsen Sea (Venables et al., 2013; Schofield et al., 2015; Oliver et al., 2019; St-Lauernt et al., 2018). The growth rate of primary production in bioregion 3 was larger than that in bioregions 5 and 8. This primary production rise accelerated before 2000, while after 2000, no significant long-term change was observed in bioregion 3. Primary production rose with fluctuations in bioregion 5 and reached a maximum in 2005. The decadal and long-term changes in primary production recorded in bioregions 3 and 5 were thought to be related to changes in dissolved iron. The correlation coefficients between primary production

https://doi.org/10.5194/bg-2021-296
Preprint. Discussion started: 11 November 2021

and dissolved iron were 0.96 in bioregion 3 and 0.59 in bioregion 5, indicating that dissolved iron was an important factor limiting primary productivity. The dissolved iron concentrations in bioregions 8 and 9 were the highest in the Amundsen Sea area (Figure 5), so dissolved iron was not the limiting factor for primary productivity in these two bioregions. The spatial differences in the limitation of dissolved iron on the primary productivity of the Amundsen Sea were consistent with previous results (Gerringa et al., 2012; Yager et al., 2012; Alderkamp et al., 2015). We also found that the primary production was significantly positively correlated with nitrate, phosphate, and silicate in bioregions 3 and 5. The correlation coefficients were all larger than 0.6 in bioregions 3 and 5. The changes in nitrate, phosphate, and silicate may have also contributed to the observed decadal and long-term changes in primary productivity. However, the Southern Ocean is the largest high-nutrient region (Lee et al., 2012). And the differences in nitrate, phosphate, and silicate were quite small among these four bioregions. So compared with bioregion 8 and 9, the nitrate, phosphate, and silicate were not thought to be limiting factors of primary productivity in bioregions 3 or 5.

4. Conclusion

The Amundsen Sea is one of the least-studied regions in the Southern Ocean and has significant spatial differences in primary productivity. In this work, we used bioregionalization to provide a basis for understanding the temporal and spatial variations in primary productivity in the Amundsen Sea.

https://doi.org/10.5194/bg-2021-296
Preprint. Discussion started: 11 November 2021

412 The spatial differences were quite significant in the Amundsen Sea; in most areas, the
413 mean primary production was less than 3 mgC m^{-3} day^{-1}. However, near the coast of
414 Pine Island Bay, mean primary production reached 14 mgC m^{-3} day^{-1}. The annual mean
415 primary production showed an increasing trend from 2013 to 2015. Primary production
416 exhibited clear seasonal variabilities and was largest in December at approximately 10
417 mgC m^{-3} day^{-1}.
418 A pelagic bioregional map of the Amundsen Sea was obtained using cluster analysis.
419 The Amundsen Sea was divided into 9 bioregions using hierarchical clustering and the
420 *K*-means clustering method. The key properties of bioregions were characterized using
421 different parameters. All bioregions had biophysical significance and could reflect
422 spatial differences in physical and ecological characteristics, such as the topography,
423 currents, upwelling, and Ross Gyre. Furthermore, the obtained bioregions could also be
424 used for systematic conservation planning of marine protected areas (MPAs) in the
425 Amundsen Sea.
426 Bioregions 3, 5, 8, and 9 were selected to analyze variations in primary productivity in
427 the Amundsen Sea. The phenology changed in bioregions 3 and 5, and these changes
428 were thought to be related to changes in dissolved iron, nitrate, phosphate, and silicate.
429 Primary production showed positive linear trends in these four bioregions. Bioregion 9
430 had the fastest growth rate, and this trend was significantly positively correlated with
431 changes in the summer sea surface temperatures. In bioregion 8, the interannual and
432 decadal variations in primary production were also positively correlated with the sea
433 surface temperatures in summer. The long-term primary changes recorded in bioregions

https://doi.org/10.5194/bg-2021-296
Preprint. Discussion started: 11 November 2021

3 and 5 were thought to be related to changes in the dissolved iron concentrations, indicating that dissolved iron was the limiting factor for primary productivity in these two bioregions.

Above results indicated that in addition to be used in the systematic conservation planning of marine protected areas, bioregionalization is also an effective method to disentangle multiple limiting factors that affect spatial differences, the phenology, decadal and long-term changes in the physical and ecological variables, such as the primary productivity.

Data availability

The Global Ocean Reanalysis and Simulation Version 4 (GLORYS2v4) dataset can be accessed from https://resources.marine.copernicus.eu/?option=com_csw&task=results&pk_vid=f205f72451b76b161622075614d28a7a.

Author contributions

JF wrote the first version of the manuscript, DL performed addition analyses, JZ made figures, and LZ revised the text.

Competing interests

The authors declare that they have no conflict of interest.

https://doi.org/10.5194/bg-2021-296
Preprint. Discussion started: 11 November 2021

Acknowledgment

This study was supported by impact and response of Antarctic seas to climate change under contract RFSOCC2020-2022-No.18, and National Science Foundation of Tianjin (19JCZDJC40600).

References

Alderkamp, A. C., van Dijken, G. L., Lowry, K. E., Connelly, T. L., Lagerström, M., Sherrell, R. M., Haskins, C., Rogalsky, E., Schofield, O., Stammerjohn, S. E., Yager, P. L., Arrigo, K. R. 2015. Fe availability drives phytoplankton photosynthesis rates during spring bloom in the Amundsen Sea Polynya, Antarctica. Elementa: Science of the Anthropocene, 3: 000043

Amthor, J. S., Baldocchi, D. D. 2001. Terrestrial Higher Plant Respiration and Net Primary Production. In Terrestrial Global Productivity, Academic Press, 33-59

Ardyna, M., Claustre, H., Sallée, J. B., D'Ovidio, F., Gentili, B., van Dijken, G., D'Ortenzio, F., Arrigo, K. R. 2017. Delineating environmental control of phytoplankton biomass and phenology in the Southern Ocean. Geophysical Research Letters, 44, 5016-5024.

Arneborg, L., Wåhlin, A. K., Björk, G., Liljebladh, B., Orsi, A. H. 2012. Persistent inflow of warm water onto the central Amundsen shelf. Nature Geoscience, 5(12): 876−880

Arrigo, K. R., van Dijken, G. L. 2003. Phytoplankton dynamics within 37 Antarctic

https://doi.org/10.5194/bg-2021-296
Preprint. Discussion started: 11 November 2021

473 coastal polynya systems. J. Geophy. Res. 108:C83271. doi:10.1029/2002JC001739

474 Arrigo, K. R., van Dijken, G. L., Bushinsky, S. 2008. Primary production in the
475 Southern Ocean, 1997-2006. Journal of Geophysical Research, 113, C08004

476 Arrigo, K. R., Lowry, K. E., van Dijken, G. L. 2012. Annual changes in sea ice and
477 phytoplankton in polynyas of the Amundsen Sea, Antarctica. Deep Sea Research Part
478 II: Topical Studies in Oceanography, 71-76, 5-15.

479 Arrigo, K. R., van Dijken, G. L., Strong, A. L. 2015. Environmental controls of marine
480 productivity hot spots around Antarctica. Journal of Geophysical Research: Oceans,
481 120(8), 5545-5565.

482 Behrenfeld, M., and E. Boss (2014), Resurrecting the ecological underpinnings of
483 ocean plankton blooms, Annu. Rev. Mar. Sci., 6, 167–194.

484 Bijma, J., Pörtner, H. O., Yesson, C., Rogers, A. D. 2013. Climate change and the
485 oceans – what does the future hold? Marine Pollution Bulletion, 74(2): 495-505.

486 Bloomfield, N. J., Knerr, N., Encinas-Viso, F. (2018). A comparison of network and
487 clustering methods to detect biogeographical regions. Ecography, 41, 1-10.

488 Bowman, J. S., Kavanaugh, M. T., Donsy, S. C., Ducklow, H. W. (2018). Recurrent
489 seascape units identify key ecological processes along the western Antarctic Peninsula.
490 Global Change Biology, 24(7), 3065-3078.

491 Boyd, P. W. (2002), Environmental factors controlling phytoplankton processes in the
492 Southern Ocean, J. Phycol., 38(5), 844–861

493 Bromwich, D. H., Nicolas, J. P., Monaghan, A. J., Lazzara, M .A., Keller, L. M.,
494 Weidner, G. A., Wilson, A. B. 2013. Central West Antarctica among the most rapidly

https://doi.org/10.5194/bg-2021-296
Preprint. Discussion started: 11 November 2021

495 warming regions on Earth. Nature Geoscience, 6, 139-145

496 Comiso, J. C., Cavalieri, D. J., Markus, T. 2003. Sea ice concentration, ice temperature,
497 and snow depth using AMSR-E data. IEEE Transactions on Geoscience & Remote
498 Sensing, 41(2): 243−252.

499 Costello, M.J. 2009. Distinguishing marine habitat classification concepts for
500 ecological data management. Mar. Ecol. Prog. Ser. 397, 253e268. http://
501 dx.doi.org/10.3354/meps08317

502 D'Ortenzio, F., and M. Ribera d'Alcalà (2009), On the trophic regimes of the
503 Mediterranean Sea: A satellite analysis, Biogeosciences, 6(2),139–148.

504 Dotto, T. S., Garabato, A. N., Bacon, S., Tsamados, M., Holland, P. R., Hooley, J.,
505 Frajka-Williams, E., Ridout, A., Meredith, M. P. 2018. Variability of the Ross Gyre,
506 Southern Ocean: drivers and responses revealed by satellite altimetry. Geophysical
507 Research Letters, 45(12): 6195−6201

508 Ebach, M. C., Murphy, D. J., Gonzalez-Orozco, C., Miller, J. 2015.A revised area
509 taxonomy of phytogeographical regions within the Australian bioregionalisation atlas.
510 Phytotaxa, 208(4), 261-277.

511 Fraley, C., Raftery, A. 1998. How many clusters? Which clustering method? Answers
512 via model-based cluster analysis. The Computer Journal, 41: 578–588.

513 Fraschetti, S., Terlizzi, A., Boero, F. 2008. How many habitats are there in the sea (and
514 where)? J. Exp. Mar. Bio. Ecol. 366, 109e115. http://dx.doi.org/10.1016/
515 j.jembe.2008.07.015

516 Gerringa, L. J. A., Alderkamp, A. C., Laan, P., Thuróczy, C. E., De Baar, H. J. W., Mills,

https://doi.org/10.5194/bg-2021-296
Preprint. Discussion started: 11 November 2021

517 M. W., van Dijken, G. L., van Haren, H., Arrigo, K. R. 2012. Iron from melting glaciers
518 fuels the phytoplankton blooms in Amundsen Sea (Southern Ocean); iron
519 biogechemistry. Deep-Sea Res Pt II , 71–76: 16–31.
520 Godet, C., Robuchon, M., Leroy, B., Cotté, C., Baudena, A., Silva, O. D., Fabri-Ruiz,
521 S., Monaco, C. L., Sergi, S., Koubbi, P. 2020. Matching zooplankton abundance and
522 environment in the South Indian Ocean and Southern Ocean. Deep Sea Research Part
523 I: Oceanographic Research Papers. 163, 103347
524 Gohl, K. 2010. The expedition of the Research Vessel Polarstern to the Amundsen Sea,
525 Antatctica, in 2010 (ANT-XXIV/3). Rep. Polar Mar. Res., 617, 173.
526 Grant, S., Constable, A., Raymond, B., Doust, S. 2006. Bioregionalisation of the
527 Southern Ocean. Report of an expert workshop, Hobart, Australia, September 2006.
528 World Wildlife Fund–Australia and Antartic Climate and Ecosystems Cooperative
529 Research Centre, 2006.
530 Grantham, H.S., Pressey, R.L., Wells, J.A., Beattie, A.J. 2010. Effectiveness of
531 biodiversity surrogates for conservation planning: different measures of effectiveness
532 generate a kaleidoscope of variation. PLoS One 5. http://dx.doi.org/10.1371/
533 journal.pone.0011430
534 Greger, E. J., Bodtker, K. M. 2007. Adaptive classification of marine ecosystems:
535 Identifying biological meaningful regions in the marine environment. Deep-Sea
536 Research I, 54, 385-402.
537 Griffiths H.J. 2010. Antarctic marine biodiversity—what do we know about the
538 distribution of life in the Southern Ocean?. PLoS One 5, e11683

https://doi.org/10.5194/bg-2021-296
Preprint. Discussion started: 11 November 2021

539 Herraiz-Borreguero, L., Lannuzel, D., van der Merwe, P., Treverrow, A., Pedro, J. B.
540 2016. Large flux of iron from the Amery Ice Shelf marine ice to Prydz Bay, East
541 Antarctica. J. Geophys.Res. Oceans, 121, 6009–6020, doi:10.1002/2016JC011687.
542 Huang, J., Zhang, Z., Wang, X. 2020. Evaluation of four high-resolution sea ice
543 reanalysis products in the Ross Sea and Amundsen Sea. Chinese Journal of Polar
544 Research, 32(4), 452-468 (In Chinese with English abstract)
545 Khatiwala, S., F. Primeau, and T. Hall (2009), Reconstruction of the history of
546 anthropogenic CO2 concentrations in the ocean, Nature, 462 (7271), 346–349.
547 Kim, C. S., Kim, T. W., Cho, K. H., Ha, H. K., Lee, S. H., Kim, H. C., Lee, J. H. 2016.
548 Variability of the Antarctic coastal current in the Amundsen Sea. Estuarine, Coastal and
549 Shelf Science, 181(5), 123-133.
550 Kim, S. U., Kim, K. Y. 2021. Impact of climate change on the primary production and
551 related biogeochemical cycles in the coastal and sea ice zone of the Southern Ocean.
552 Science of The Total Environment, 751, 141678.
553 Koubbi, P., Moteki, M., Duhamel, G., Goarant, A., Hulley, P.A., O'Driscoll, R.,
554 Ishimaru, T., Pruvost, P., Tavernier, E., Hosie, G., 2011. Ecoregionalization of
555 myctophid fish in the Indian sector of the Southern Ocean: results from generalized
556 dissimilarity models. Deep. Res. Part II Top. Stud. Oceanogr. 58, 170e180.
557 http://dx.doi.org/10.1016/j.dsr2.2010.09.007
558 Kulkarni, A.; von Storch, H. 1995. Monte Carlo experiments on the effect of serial
559 correlation on the Mann-Kendall-test of trends. Meteor Z. 4, 82–85
560 Kwon, Y. S., La, H. S., Jung, J., Lee, S. H., Kim, T. W., Kang, H. W., & Lee, S. H.

https://doi.org/10.5194/bg-2021-296
Preprint. Discussion started: 11 November 2021

(2021). Exploring the Roles of Iron and Irradiance in Dynamics of Diatoms and Phaeocystis in the Amundsen Sea Continental Shelf Water. Journal of Geophysical Research: Oceans, 126(3), 1-23.

Lacour, L., H. Claustre, L. Prieur, and F. D'Ortenzio (2015), Phytoplankton biomass cycles in the North Atlantic subpolar gyre: A similar mechanism for two different blooms in the Labrador Sea, Geophys. Res. Lett., 42, 5403–5410, doi:10.1002/2015GL064540.

Lannuzel, D., Schoemann, V., De Jong, J., Tison, J. L., Chou, L. 2007. Distribution and biogeochemical behaviour of iron in the East Ant-arctic sea ice. Mar. Chem, 106(1), 18–32.

Leathwick, J. R., Overton, J., McLeod, M. 2003. An environmental domain classification of New Zealand and its use as a tool for biodiversity management. Conservation Biology 17: 1612–1623.

Lee, S. H., Kim, B. K., Yun, M. S., Joo, H., Yang, E. J., Kim, Y. N., Shin, H. C., Lee, S. 2012. Spatial distribution of phytoplankton productivity in the Amundsen Sea, Antarctica. Polar Biology, 35, 1721-1733.

Lim, Y. J., Kim, T. W., Lee, S., Lee, D., Park, J., Kim, B .K., Kim, K., Jang, H. K., Bhavya, P. S., Lee, S. H. 2019. Seasonal variations in the small phytoplankton contribution to the total primary production in the Amundsen Sea, Antarctica. Journal of Geophysical Research, Oceans. 124(11), 8324-8341.

Longhurst, A. (2007), Ecological Geography of the Sea, 2nd ed., p. 542, Academic Press, Burlington, Mass.

https://doi.org/10.5194/bg-2021-296
Preprint. Discussion started: 11 November 2021

583 Ma, H., Wang, Z., Shi, J. 2012. The Role of the Southern Ocean Physical Processes in
584 Global Climate System. Advances in Earth Science, 27(4): 398-412.
585 Mann, H. B. 1945. Nonparametric tests against trend. Econometrica, 13, 245-259.
586 Martinson, D. G. 2012. Antarctic circumpolar current's role in the Antarctic ice system:
587 An overview. Palaeogeography, Palaeoclimatology, Palaeoecology, 335-336: 71−74
588 Mayot, N., F. D'Ortenzio, M. Ribera d'Alcalà, H. Lavigne, and H. Claustre (2016),
589 Interannual variability of the Mediterranean trophic regimes from ocean color satellites,
590 Biogeosciences, 13(6), 1901–1917.
591 Meier, W. N., Fetterer, F., Savoie, M., Mallory, S., Duerr, R., Stroeve, J. 2017.
592 NOAA/NSIDC Climate Data Record of Passive Microwave Sea Ice Concentration,
593 Version 3. Boulder, Colorado USA. NSIDC: National Snow and Ice Data Center. doi:
594 https://doi.org/10.7265/N59P2ZTG.
595 Milligan, G. W., Cooper, M. C. 1987. Methodology review: clustering methods. – Appl.
596 Psychol. Meas. 11: 329–354.
597 Moore, J. K., Abbott, M. R. 2000. Phytoplankton chlorophyll distributions and primary
598 production in the Southern Ocean, J. Geophys. Res., 105(C12), 28, 709-722,
599 doi:10.1029/1999JC000043.
600 Oliver, M. J., Irwin, A. J. 2008. Objective global ocean biogeographic provinces.
601 Geophys. Res. Lett. 35, L15601
602 Oliver, H., St‐Laurent, P., Sherrell, R. M., Yager, P. L. 2019. Modeling Iron and Light
603 Controls on the Summer Phaeocystis antarctica Bloom in the Amundsen Sea Polynya.
604 Global Biogeochemical Cycles, 33(5), 570-596.

https://doi.org/10.5194/bg-2021-296
Preprint. Discussion started: 11 November 2021

605 Pabis, K., Błażewicz, M., Jóźwiak, P., Barnes, D. K.A. 2015. Tanaidacea of the
606 Amundsen and Scotia Seas: an unexplored diversity. Antarctic Science, 27(1):19-30.
607 Palmiéri, J., Dutay, J. C., D'Ortenzio, F., Houpert, L., Mayot, N., Bopp, L. (2018). The
608 Mediterranean subsurface phytoplankton dynamics and their impact on Mediterranean
609 bioregions. Biogeosciences Discuss., https://doi.org/10.5194/bg-2018-423
610 Park, K., Hahm, D., Choi, J. O., Xu, S., Kim, H. C., Lee, S. H. 2019. Spatiotemporal
611 variation in summer net community production in the Amundsen Sea Polynya: A self-
612 organizing map analysis approach. Continental Shelf Research, 184, 21-29.
613 Park, J., Kuzminovm, F. I., Bailleul, B., Yang, E. J., Lee, S., Falkowski, P .G., Gorbunov,
614 M. Y. 2017. Light availability rather than Fe controls the magnitude of massive
615 phytoplankton bloom in the Amundsen Sea polynyas, Antarctica. Limnology and
616 Oceanography, 62(5): 2260-2276.
617 Petrou, K., Kranz, S. A., Trimborn, S., Hassler, C. S., Ameijeiras, S. B., Sackett, O.,
618 Ralph, P. J., Davidson, A. T. 2016. Southern Ocean phytoplankton physiology in a
619 changing climate. J. Plant. Physiol. 20, 203, 135-150.
620 Reid, P.C., Fischer, A.C., Lewis-Brown, E., Meredith, M.P., Sparrow, M., Andersson,
621 A.J., Antia, A., Bates, N.R., Bathmann, U., Beaugrand, G., Brix, H., Dye, S., Edwards,
622 M., Furevik, T., Gangstø, Hátún, H., Hopcroft, R.R., Kandall, M., Kasten, S., Keeling,
623 R., LeQuéré, C., Mackenzie, F.T., Malin, G., Mauritzen, C.,Ólafsson, J., Paull, C.,
624 Rignot, E., Shimada, K., Vogt, M., Wallace, C., Wang, Z., Washington, R. 2009.
625 Impacts of the oceans on climate change. Advances in Marine Biology, 56: 1-150
626 Rice, J., Gjerde, K.M., Ardron, J., Arico, S., Cresswell, I., Escobar, E., Grant, S.,

https://doi.org/10.5194/bg-2021-296
Preprint. Discussion started: 11 November 2021

627 Vierros, M., 2011. Policy relevance of biogeographic classification for conservation
628 and management of marine biodiversity beyond national jurisdiction, and the GOODS
629 biogeographic classification. Ocean. Coast. Manag. 54, 110e122.
630 http://dx.doi.org/10.1016/j.ocecoaman.2010.10.010
631 Ritterhoff, J., Zauke, G.P. 1997. Trace metals in field samples of zooplankton from the
632 Fram Strait and the Greenland Sea, Sci. Total Environ., 199, 255–270,
633 doi:10.1016/S0048-9697(97)05457-0
634 Roberson, L. A., Lagabrielle, E., Lombard, A. T., Sink, K., Livingstone, T., Grantham,
635 H., Harris, J. M. 2017. Pelagic bioregionalisation using open-access data for better
636 planning of marine protected area networks. Ocean & Coastal Management, 148, 214-
637 230.
638 Schofield, O. M., Miles, T., Alderkamp, A.-C., Lee, S., Haskins, C., Rogalsky, E., et al.
639 2015. In situ phytoplankton distributions in the Amundsen Sea Polynya measured by
640 autonomous gliders. Elementa: Science of the Anthropocene, 3, 000073.
641 Sharp, B. R., Parker, S. J., Pinkerton, M., Breen, B. A., Cummings, V. J., Dunn, A.,
642 Grant, S. M., Hanchet, S., Keys, H. J. R., Lockhart, S. J., Lyver, P., O'Driscoll, R. L.,
643 Williams, M., Wilson, P. R. 2010. Bioregionalisation and Spatial Ecosystem Processes
644 in the Ross Sea Region. Document WG-EMM-10/30. Hobart, TAS: CCAMLR.
645 Smith, W. O., Jr., Comiso, J. C. 2008. Influence of sea ice on primary production in the
646 Southern Ocean, A satellite perspective. Journal of Geophysical Research, Oceans, 113,
647 C05S93.
648 Snelder, T. H., Leathwick, J., Dey, K., Rowden, A. A., Weatherhead, M. A., Fenwick,

https://doi.org/10.5194/bg-2021-296
Preprint. Discussion started: 11 November 2021

649 G. D., Francis, M. P., Gorman, R. M., Grieve, J. M., Hadfield, M .G., Hewitt, J. E.,
650 Richardson, K. M., Uddstrom, M. J., Zeldis, J. R. 2007. Development of an
651 ecological marine classification in the New Zealand region.
652 Environmental Management 39: 12–29

653 Spalding, M.D., Fox, H.E., Allen, G.R., Davidson, N., FerdaNa, Z., Finlayson, M.,
654 Halpern, B.S., Jorge, M.A., Lombana, A.L., Lourie, S.A., Martin, K.D., McManus, E.,
655 Molnar, J., Recchia, C.A., Robertson, J. 2007. Marine ecoregions of the world: a
656 bioregionalization of coastal and shelf areas. Bioscience 57, 573-583. http://
657 dx.doi.org/10.1641/B570707

658 Stammerjohn, S. E., Maksym, T., Lowry, K. E., Arrigo, K. R., Yuan, X., Raphael, M.,
659 Randall-Goodwin, E., Sherrell, R. M., Yager, P. L. 2015. Seasonal sea ice changes in
660 the Amundsen Sea, Antarctica, over the period of 1979-2014. Elementa: Science of the
661 Anthropocene. 3: 000055.

662 St-Laurent, P., Yager, P. L., Sherrell, R. M., Stammerjohn, S. E., Dinniman, M. S. 2017.
663 Pathways and supply of dissolved iron in the Amundsen Sea (Antarctica). Journal of
664 Geophysical Research: Oceans, 122(9): 7135−7162.

665 St-Laurent, P., Yager, P. L., Sherrell, R. M., Oliver, H., Dinniman, M. S., &
666 Stammerjohn, S. E. 2019. Modeling the Seasonal Cycle of Iron and Carbon Fluxes in
667 the Amundsen Sea Polynya, Antarctica. Journal of Geophysical Research: Oceans,
668 124(3), 1544-1565

669 Swalethorp, R., Dinasquet, J., Logares, R., Bertilsson, S., Kjellerup, S., Krabberød, A.
670 K., Moksnes, P. O., Nielsen, T. G., Riemann, L. 2019. Microzooplankton distribution

https://doi.org/10.5194/bg-2021-296
Preprint. Discussion started: 11 November 2021

671 in the Amundsen Sea Polynya (Antarctica) during an extensive Phaeocystis antarctica
672 bloom. Progress in Oceanography, 170, 1-10.
673 Teschke, K., Beaver, D., Bester, M. N., et al. 2016. Scientific background document in
674 support of the development of a CCAMLR MPA in the Weddell Sea (Antarctica)—
675 version 2016—part A: general context of the establishment of MPAs and background
676 information on the Weddell Sea MPA planning area. CCAMLR. 2016, 1–112.
677 Treml, E.A., Halpin, P.N., 2012. Marine population connectivity identifies ecological
678 neighbors for conservation planning in the Coral Triangle. Conserv. Lett. 5, 441-449.
679 http://dx.doi.org/10.1111/j.1755-263X.2012.00260.x.
680 Twelves, A. G., Goldberg, D. N., Henley, S. F., Mazloff, M. R., & Jones, D. C. 2021.
681 Self-Shading and Meltwater Spreading Control the Transition From Light to Iron
682 Limitation in an Antarctic Coastal Polynya. Journal of Geophysical Research: Oceans,
683 126(2), 1-28.
684 Uotila, P., Goosse, H., Haines, K., Chevallier, M., Barthélemy, A., Bricaud, C., Carton,
685 J., Fučkar, N., Garric, G., Iovino, D., Kauker, F., Korhonen, M., Lien, V. S., Marnela,
686 M., Massonnet, F., Mignac, D., Peterson, K. A., Sadikni, R., Shi, L., Tietsche, S.,
687 Toyoda, T., Xie, J., and Zhang, Z. 2019. An assessment of ten ocean reanalyses in the
688 polar regions, Clim. Dynam., 52, 1613–1650, https://doi.org/10.1007/s00382-018-
689 4242-z.
690 Venables, H. J., Clarke, A., Mereddith, M. P. 2013. Wintertime controls on summer
691 stratification and productivity at the Western Antarctic Peninsula. Limnology and
692 Oceanography, 58:1035-1047.

https://doi.org/10.5194/bg-2021-296
Preprint. Discussion started: 11 November 2021

693 Wu, S. Y., Hou, S. 2017. Impact of icebergs on net primary productivity in the Southern
694 Ocean[J], The Cryosphere, 11, 707–722, https://doi.org/10.5194/tc-11-707-2017
695 Yager, P., Sherrell, R. M., Stammerjohn, S. E., Alderkamp, A. C., Schofield, O.,
696 Abrahamsen, E.P., Arrigo, K.R., Bertilsson, S., Garay, D.L., Guerrero, R., Lowry, K.E.,
697 Moksnes, P.-O., Ndungu, K., Post, A.F., Randall-Goodwin, E., Riemann, L., Severmann,
698 S., Thatje, S., van Dijken, G.L., Wilson, S. 2012. ASPIRE: The Amundsen Sea Polynya
699 International Research Expedition. Oceanography, 25: 40–53.

700

701 **Tables:**

702 Table 1. Variables from GLORYS2V4 used in pelagic bioregionalization

Physical	**Biological**
Temperature (*tem*) Salinity (*sal*) Sea surface height (*ssh*) Density ocean mixed layer thickness (*mlp*) Sea floor potential temperature (*bot*) Ice concentration (*fice*)	Total Chlorophyll (*chl*) Total primary production of phytoplankton (*nppv*) Dissolved Iron (*fe*)

703

704

705

https://doi.org/10.5194/bg-2021-296
Preprint. Discussion started: 11 November 2021

706

707 Table 2. Mean values of variables at different bioregions.

	ALL	6-6	9-8	9-9	6-3	9-4	9-7
tem (K)	273.86	271.56	271.53	271.57	276.42	277.07	276.03
mlp (m)	66.66	42.71	43.51	43.14	94.69	112.43	67.24
ssh (m)	-1.25	-1.59	-1.59	-1.60	-0.43	-0.77	-1.08
bot (K)	273.46	273.34	274.06	272.97	273.33	273.32	273.63
ice	0.59	0.96	0.97	0.95	0.12	0.05	0.20
sal	33.65	33.22	33.31	33.19	33.92	33.99	33.86
chl (mg m^{-3})	0.38	0.72	0.57	0.76	0.33	0.32	0.36
nppv (mgC m^{-3} day^{-1})	3.64	8.01	5.86	8.51	2.99	3.12	3.19
fe (mmol m-3)	<0.001	0.002	0.001	0.003	<0.001	<0.001	<0.001
depth (m)	-3000	-144	-295	-86	-4448	-3276	-4613

708

709

710

711

712

https://doi.org/10.5194/bg-2021-296
Preprint. Discussion started: 11 November 2021

Biogeosciences
Discussions
Open Access
EGU

713

714 **Figures**

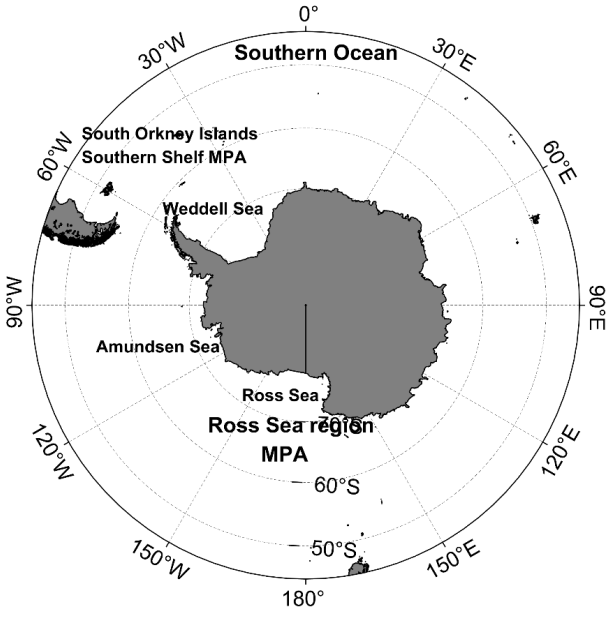

715

716 **Figure 1**. Locations of the Southern Ocean, Weddell Sea, Rose Sea, and Amundsen Sea

https://doi.org/10.5194/bg-2021-296
Preprint. Discussion started: 11 November 2021

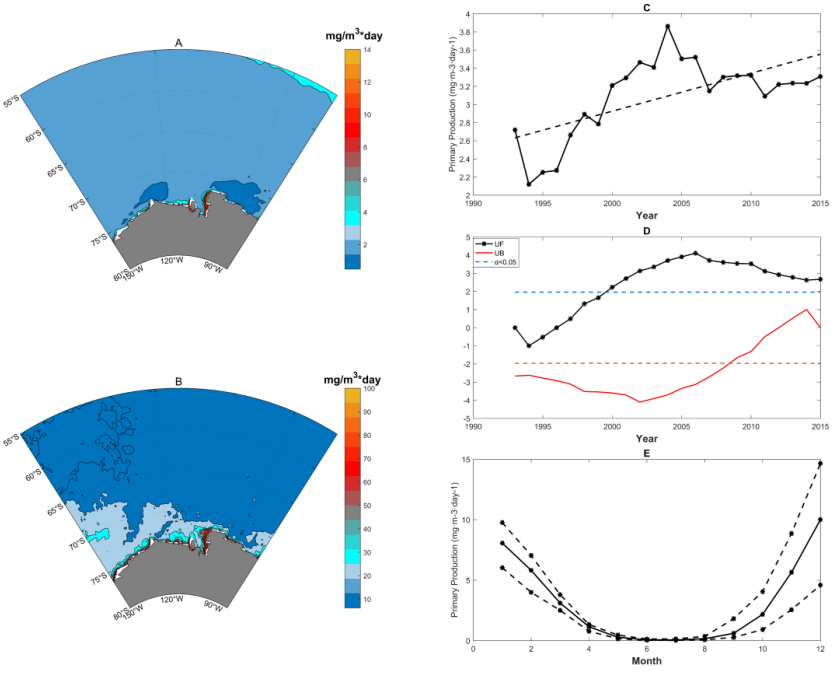

717

718 **Figure 2**. Primary production in the Amundsen Sea, (A) mean value of primary
719 production; (B) seasonality amplitude of primary production; (C) annual values of
720 (black line) and long-term changes in (black dashed line) primary production; (D) MK-
721 values (y-axes) obtained from the sequential Mann-Kendall test against time for annual
722 primary production; (E) monthly primary production values (black line) and amplitudes
723 of the monthly values (black broken line).

https://doi.org/10.5194/bg-2021-296
Preprint. Discussion started: 11 November 2021

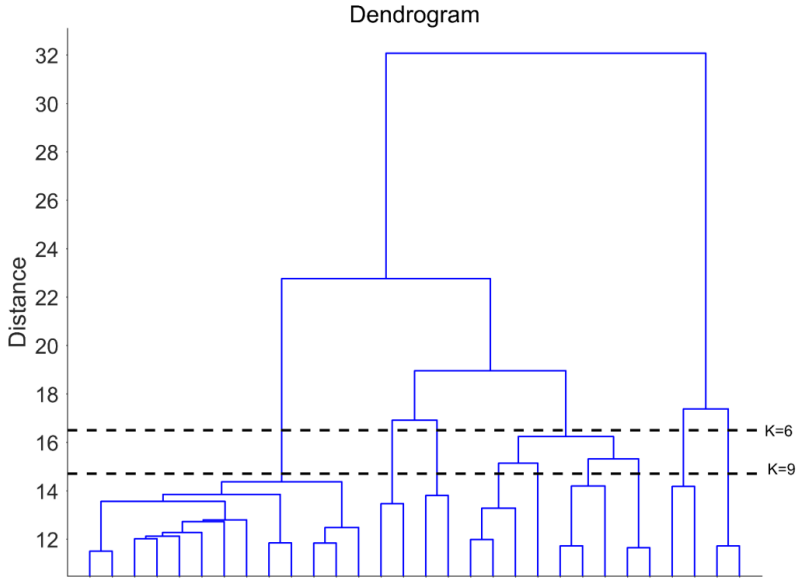

724

725 **Figure 3**. Dendrogram obtained from hierarchical clustering. The dotted lines (*K*=6 and

726 *K*=9) show the levels at which the dendrogram was cut to produce the groups.

https://doi.org/10.5194/bg-2021-296
Preprint. Discussion started: 11 November 2021

Biogeosciences
Discussions
Open Access
EGU

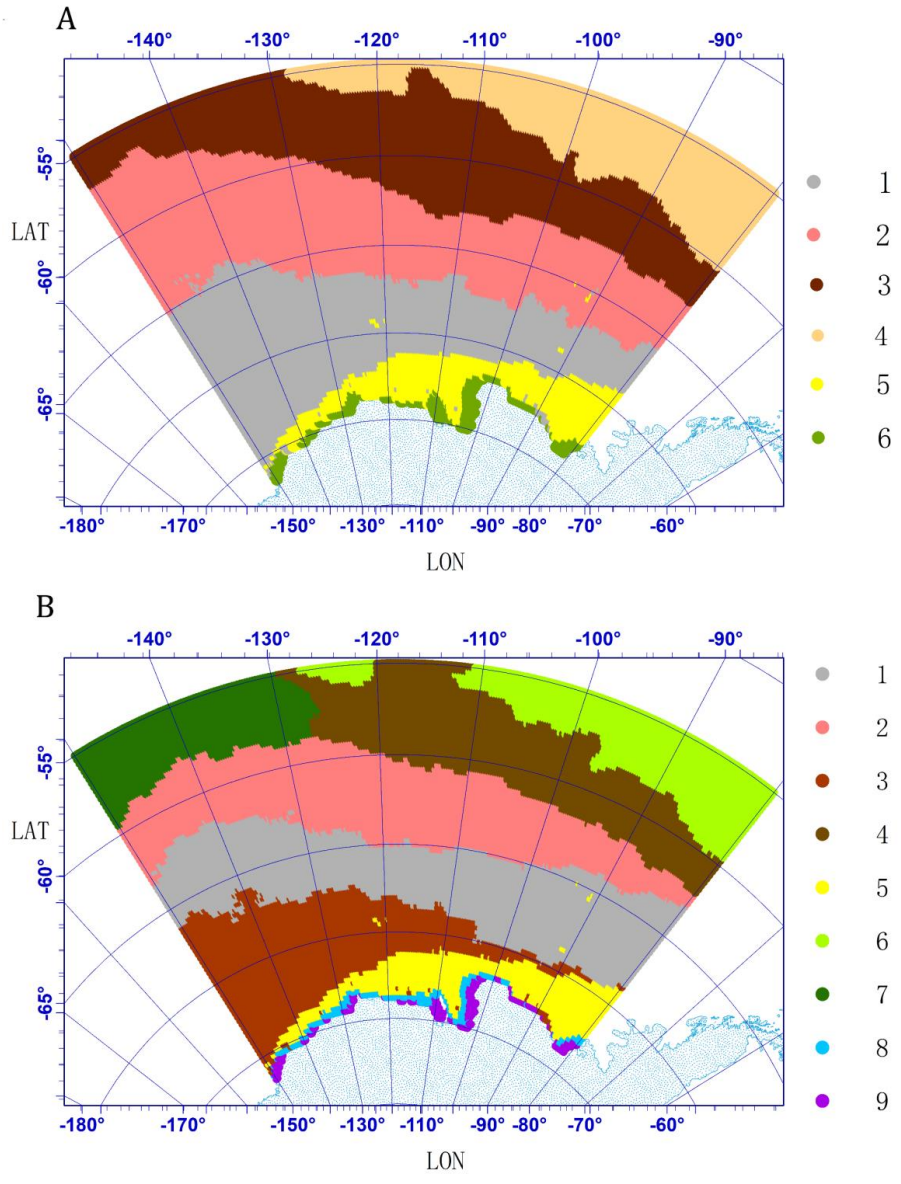

727

728 **Figure 4**. Six bioregions identified in the *K*-means cluster analysis (A); 9 bioregions

729 identified in the *K*-means cluster analysis (B)

https://doi.org/10.5194/bg-2021-296
Preprint. Discussion started: 11 November 2021

Biogeosciences
Discussions
Open Access
EGU

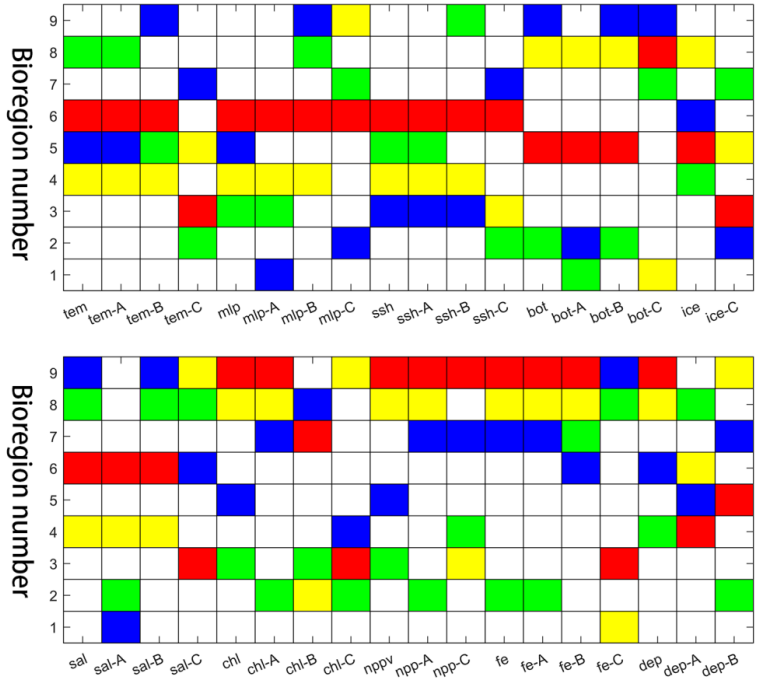

730

731 **Figure 5**. Parameters that characterize the key properties of bioregions, showing the
732 maximum value (red), the second-highest value (yellow), the minimum value (blue)
733 and the second-lowest value (green) of each parameter, including the annual maximum
734 mean (A), annual minimum mean (B), and long-term change rate (C) (dep-A: latitudinal
735 gradient, dep-B: longitudinal gradient)

https://doi.org/10.5194/bg-2021-296
Preprint. Discussion started: 11 November 2021

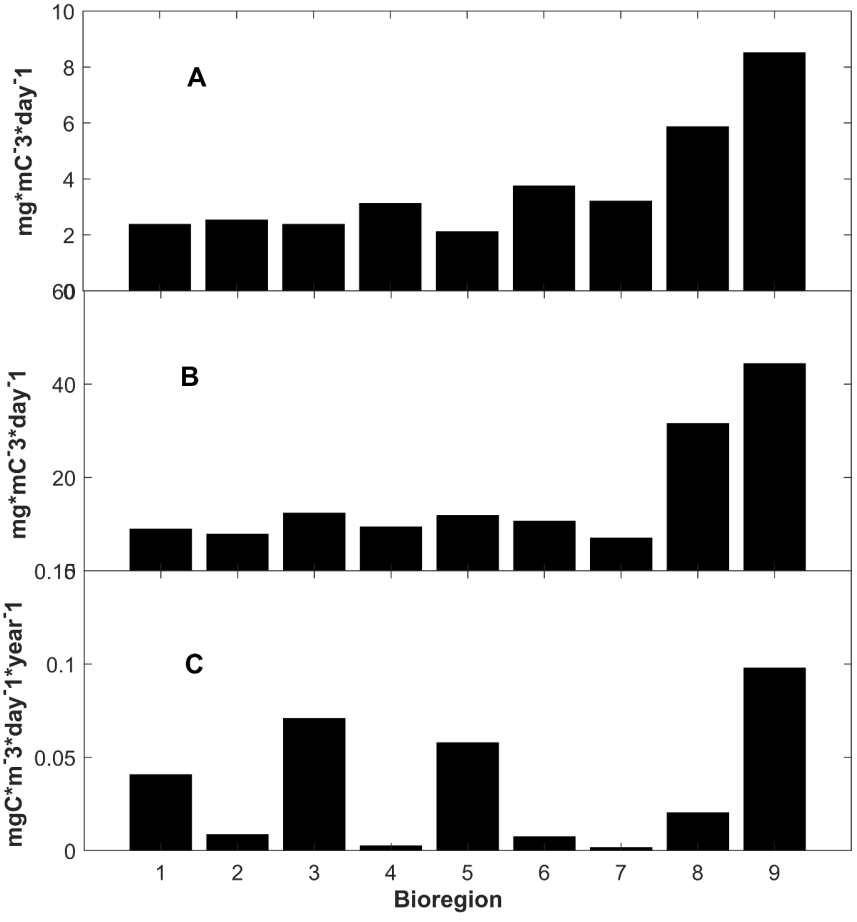

736

737 **Figure 6**. Mean values (A), annual maximum mean values (B), and long-term change

738 rates (C) of primary production in 9 bioregions.

https://doi.org/10.5194/bg-2021-296
Preprint. Discussion started: 11 November 2021

Biogeosciences
Discussions
Open Access
EGU

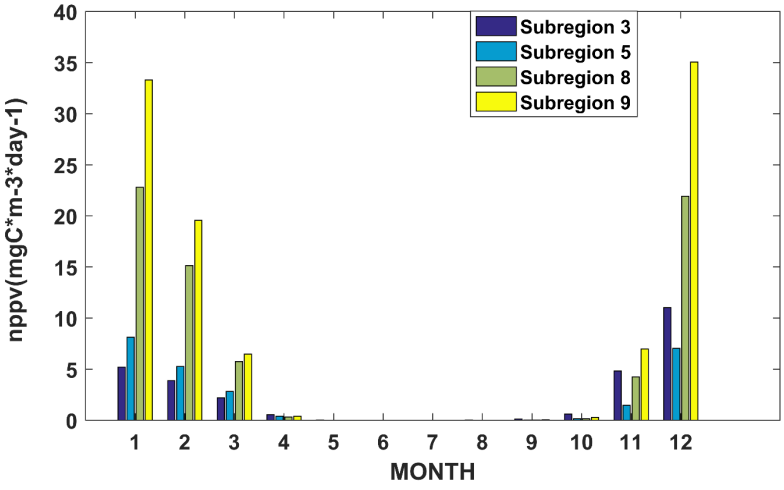

739

740 **Figure 7**. Monthly mean net primary productivity values in bioregions 3, 5, 8, and 9

741 from 1993 to 2015

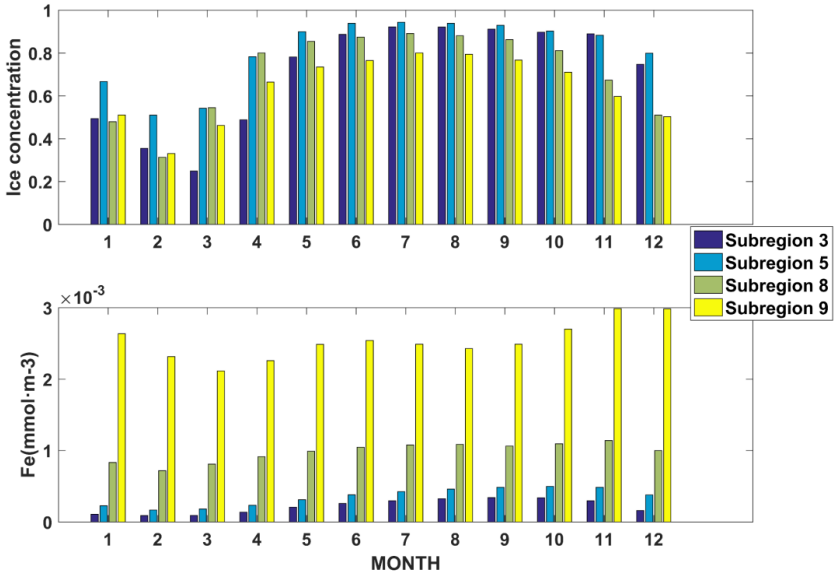

742

743 **Figure 8.** Monthly mean ice concentration and dissolved iron in bioregions 3, 5, 8, and

744 9 from 1993 to 2015.

https://doi.org/10.5194/bg-2021-296
Preprint. Discussion started: 11 November 2021

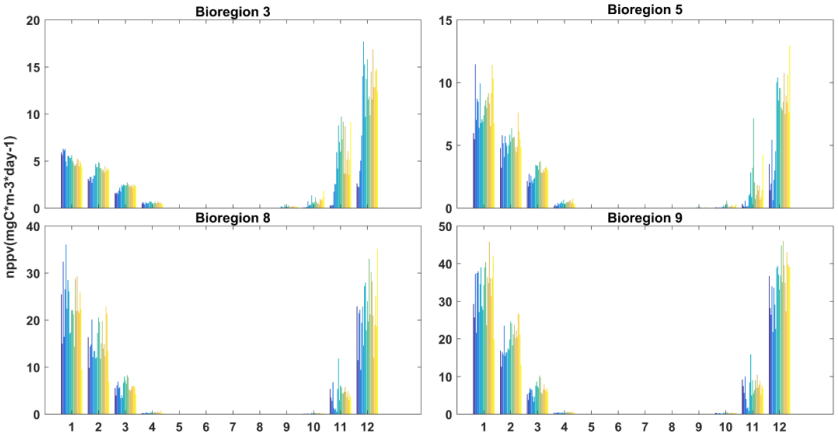

745

746 **Figure 9**. Changes in monthly net primary productivity values in bioregions 3, 5, 8,

747 and 9 from 1993 to 2015 (the colors represents different years)

https://doi.org/10.5194/bg-2021-296
Preprint. Discussion started: 11 November 2021

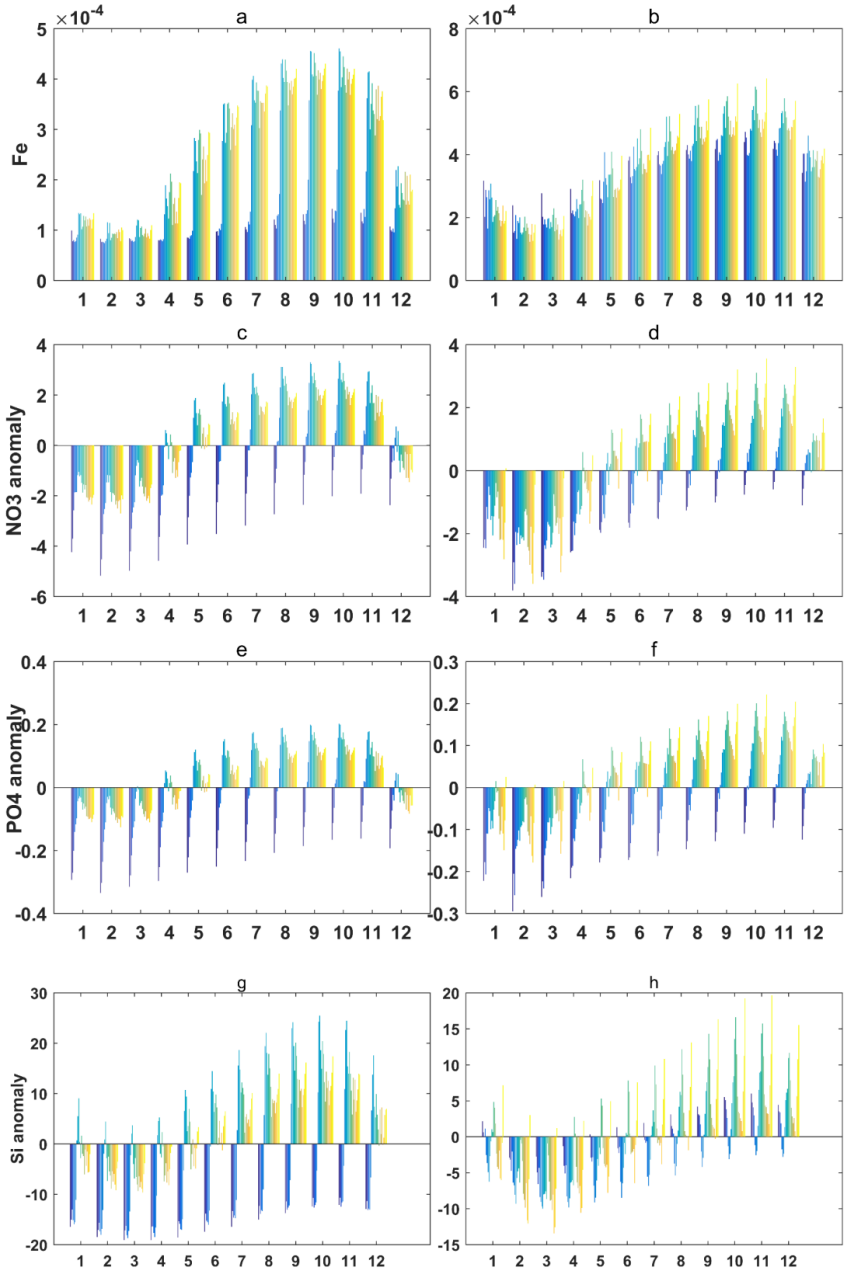

Figure 10. Changes in monthly Fe values in bioregions 3 (a) and 5 (b) from 1993 to 2015; changes in monthly nitrate anomalies in bioregions 3 (c) and 5 (d); changes in monthly phosphate anomalies in bioregions 3 (e) and 5 (f); and changes in monthly

https://doi.org/10.5194/bg-2021-296
Preprint. Discussion started: 11 November 2021

752 silicate anomalies in bioregions 3 (g) and 5 (h)

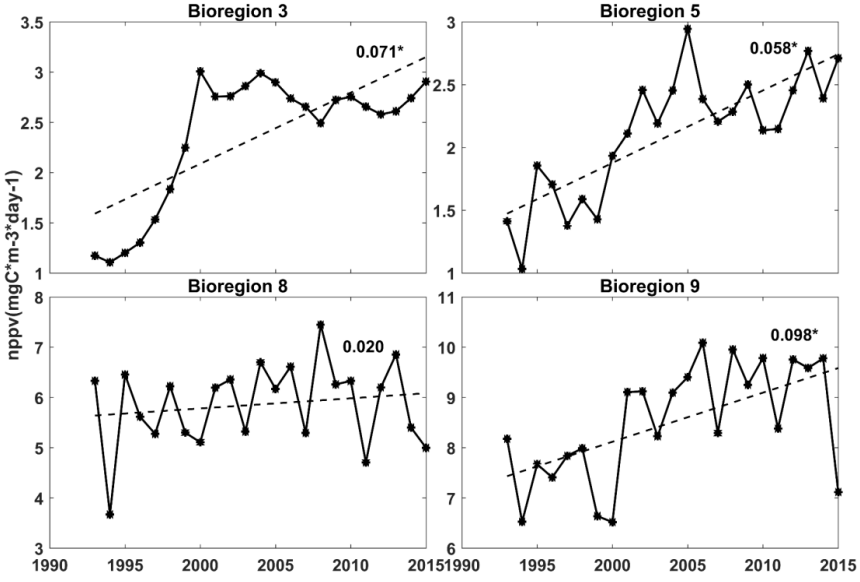

753

754 **Figure. 11.** Annual net primary productivity rates (full line) in bioregions 3, 5, 8 and 9

755 from 1993 to 2015, the dotted lines indicate the linear trends (numbers are the change

756 rates).

757